

Room temperature critical behavior and magnetocaloric properties of $\text{La}_{0.6}\text{Nd}_{0.1}(\text{CaSr})_{0.3}\text{Mn}_{0.9}\text{V}_{0.1}\text{O}_3$

A. Dhahri^{a,*}, F.I.H. Rhouma^a, S. Mnefgui^a, J. Dhahri^a, E.K. Hlil^b

^aLaboratory of Material Condensed and Nanoscience, Faculty of Sciences, University of Monastir, 5019 Monastir, Tunisia

^bInstitut Néel, CNRS-Université Joseph Fourier, Bp 166, 38042 Grenoble, France

Available online 28 June 2013

Abstract

The magnetocaloric effect along magnetic phase transition and critical exponent in mixed manganite $\text{La}_{0.6}\text{Nd}_{0.1}(\text{CaSr})_{0.3}\text{Mn}_{0.9}\text{O}_3$ was investigated by dc magnetization measurements. Magnetic data indicate that the compound exhibit a continuous (second-order) paramagnetic (PM) to ferromagnetic (FM) phase transition. From the derived values of the critical exponents ($\beta=0.385(1)$ and $\gamma=1.481(3)$), we conclude that $\text{La}_{0.6}\text{Nd}_{0.1}(\text{CaSr})_{0.3}\text{Mn}_{0.9}\text{V}_{0.1}\text{O}_3$ belongs to the three-dimensional Heisenberg class with short-range interaction. The maximum magnetic entropy ($-\Delta S_M$) and the relative cooling power (RCP) were found to be respectively, 4.266 J/kg K and 205.35 J/kg for a 5 T field change, making of this material a promising candidate for magnetic refrigeration near room temperature. From the field dependence of RCP and ΔS_M , it was possible to evaluate the critical exponents of the magnetic phase transitions. Their values are in good agreement with those obtained from the critical exponents using a modified Arrott method.

© 2013 Elsevier Ltd and Techna Group S.r.l. All rights reserved.

Keywords: Manganites; Magnetocaloric effect; Relative cooling power; Critical exponents

1. Introduction

Recently, the perovskite manganites $\text{Re}_{1-x}\text{T}_x\text{MnO}_3$ ($\text{Re}^{3+} = \text{La}^{3+}, \text{Pr}^{3+}, \text{Nd}^{3+}$, etc.; $\text{T}^{2+} = \text{Ca}^{2+}, \text{Ba}^{2+}, \text{Sr}^{2+}$, etc.; ABO₃ type) had attracted considerable interest because they exhibit interesting physical effects and had potential applications due to the complex relationship between crystal structure, electrical, magnetic, and thermal properties, for example, the negative colossal magnetoresistance effect (CMR) and the magnetocaloric effect, the latter generally accompanied by a paramagnetic–ferromagnetic transition [1–3]. One of the effective methods is to study in detail the critical exponents associated with the transition. In an earlier theoretical, critical behavior related to the paramagnetic (PM) to ferromagnetic (FM) transition of manganite in double exchange model was described within the framework of long range mean-field theory. However, the recent theoretical calculations have predicted the critical exponents in manganites in agreement with the short-range exchange interaction model [4,5]. Critical exponents for manganites show wide variation which covers almost all the universality classes

even for the systems, when different experimental tools are used to determine them. So the interactions around the critical point will follow the scaling relations with critical exponents belonging to the conventional universality classes [6,7]. At present, the 3D Heisenberg model is extensively used to discuss critical properties and to understand short-range interaction in doped manganites [8]. A few experimental studies of critical phenomena have been previously made on same hole-doped as well as electron doped manganites [9,10]. It has been recently shown that there exists a universal curve for the magnetic entropy change for second order transition materials [11]. It can be constructed using a phenomenological procedure which does not require the knowledge of either the equation of state or the critical exponents of the material. Expressing the field dependence as ΔS_M vs. H^n , this approach allows us to find a relationship between the exponent n and the critical exponents of the material and to propose a phenomenological universal curve for the field dependence of ΔS_M , which was successfully tested for series of soft magnetic amorphous alloys and lanthanide based crystalline materials. Up to now very little attention has been paid to the field dependence of RCP [12].

$\text{La}_{0.6}\text{Nd}_{0.1}(\text{CaSr})_{0.3}\text{Mn}_{0.9}\text{O}_3$ is one of the extensively studied manganites which undergoes a paramagnetic metal to a

*Corresponding author Tel.: +216 97 281 676; fax: +216 73 500 278.

E-mail address: abdessalem_dhahri@yahoo.fr (A. Dhahri).

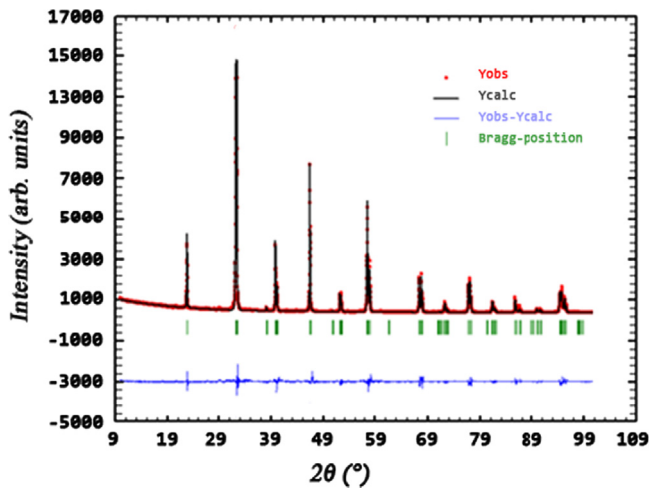


Fig. 1. X-ray diffraction pattern and the corresponding Rietveld refinement of the $\text{La}_{0.6}\text{Nd}_{0.1}(\text{CaSr})_{0.3}\text{Mn}_{0.9}\text{V}_{0.1}\text{O}_3$ sample.

ferromagnetic metal transition around $T_C = 325$ K and it shows a ΔS_M of $1.49 \text{ J kg}^{-1} \text{ K}^{-1}$ under $\mu_0 H = 1$ T around its T_C [13].

As a contribution to the investigation of manganite materials, we report here the study of the effect, on the structural, magnetic, critical phenomenal and magnetocaloric properties, of V-doping in the $\text{La}_{0.6}\text{Nd}_{0.1}(\text{CaSr})_{0.3}\text{Mn}_{0.9}\text{V}_{0.1}\text{O}_3$ polycrystalline sample.

2. Experimental details

A polycrystalline sample $\text{AMn}_{0.9}\text{V}_{0.1}\text{O}_3$ ($A = \text{La}_{0.6}\text{Nd}_{0.1}(\text{CaSr})_{0.3}$) compound were formed by a standard solid state reaction, used commercial powders ($> 99.99\%$ purity) La_2O_3 , Nd_2O_3 , CaCO_3 , SrCO_3 , V_2O_3 and MnO_2 precursors. The detailed experimental process has been reported elsewhere [14]. The structure and phase purity of the prepared samples were checked by X-ray diffraction (XRD), using $\text{Cu-K}\alpha_1$ radiation at room temperature. Magnetization vs. temperature and magnetic field curves were measured by using a Foner magnetometer equipped with a superconducting coil.

3. Results and discussion

3.1. Structural properties

Fig. 1 shows the XRD pattern after structural refinement using FULLPROF program [15], for the sample. The shifted Chebyshev polynomial with 10 variables was used to fit the background refinement and a Pseudo-Voigt function was selected to refine the shape of the peak. The analysis confirms that the structure of the compound was rhombohedral with $R\bar{3}c$ space group at room temperature and the stoichiometric nature of the sample is confirmed from the analysis. The refined lattice parameters are $a = 5.412(2) \text{ \AA}$, $c = 13.298(4) \text{ \AA}$ and $V = 347.55(2) \text{ \AA}^3$.

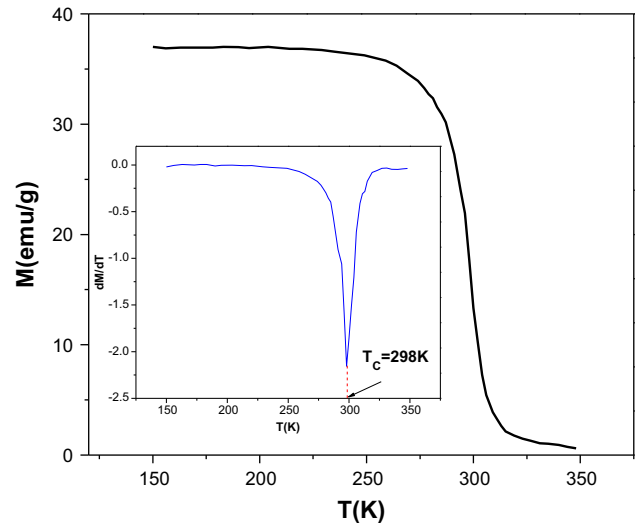


Fig. 2. Temperature dependence of magnetization under a magnetic field of 500 Oe for $\text{La}_{0.6}\text{Nd}_{0.1}(\text{CaSr})_{0.3}\text{Mn}_{0.9}\text{V}_{0.1}\text{O}_3$ sample. The inset shows the temperature derivative dM/dT with $T_C = 298$ K.

3.2. Magnetic properties

The investigation of the magnetic properties measured in a magnetic field of 500 Oe proved that the sample $\text{AMn}_{0.9}\text{V}_{0.1}\text{O}_3$ exhibit a single magnetic transition and behave in a ferromagnetic manner at a low temperature ($T \leq T_C$) and in paramagnetic manner above the Curie temperature T_C ($T \geq T_C$) as shown in Fig. 2. This result confirms well the good quality of our sample. The temperature derivative of the M - T curve is shown in the inset of Fig. 2, from which the Curie temperature T_C ($T_C = 298$ K) can be univocally determined. This value is very close to the room temperature, which is quite suitable for magnetic refrigeration.

The magnetization M as a function of the applied magnetic field, at various temperatures, is shown in Fig. 3. Characteristic $M(H)$ curves of manganites usually exhibit a very high increase in M at low fields and then a gradual saturation at high fields. The present sample also shows a steep rise in the low field range, the magnetization still increases steadily with increasing magnetic field and does not show any sign of saturation, even at 5 T. To analyze the nature of the magnetic phase transition in detail, we have carried out critical exponent study near T_C for $\text{AMn}_{0.9}\text{V}_{0.1}\text{O}_3$ sample.

3.3. Critical behavior

According to the scaling hypothesis [16], for a second order phase transition around the Curie point T_C , critical exponents β (associated with the spontaneous magnetization $M_s(H=0)$ below T_C), γ (associated with the initial susceptibility $\chi = (\partial M / \partial H)$ above T_C), and δ (associated with the critical isotherm $M(T_C, H)$ at T_C) are given as

$$M_s(T) = M_0(-t)^\beta, \quad t < 0, \quad (1)$$

$$\chi_0^{-1}(T) = \left(\frac{h_0}{M_0}\right)t^{-\gamma}, \quad t > 0 \quad (2)$$

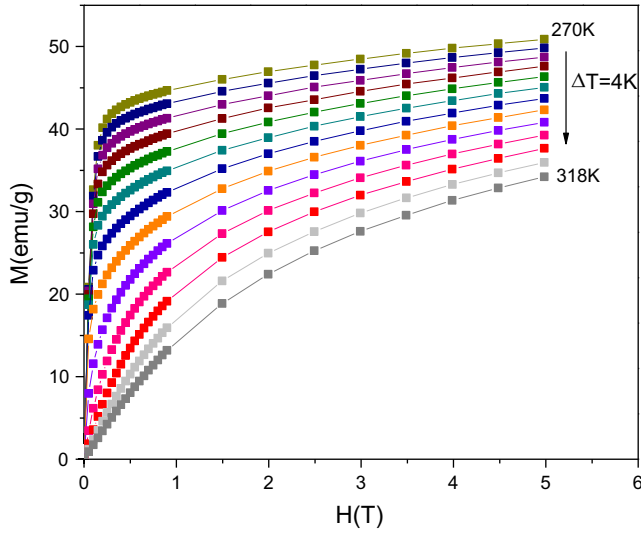


Fig. 3. Magnetization vs. applied magnetic field H , measured at different temperatures around T_C , for $\text{La}_{0.6}\text{Nd}_{0.1}(\text{CaSr})_{0.3}\text{Mn}_{0.9}\text{V}_{0.1}\text{O}_3$ sample.

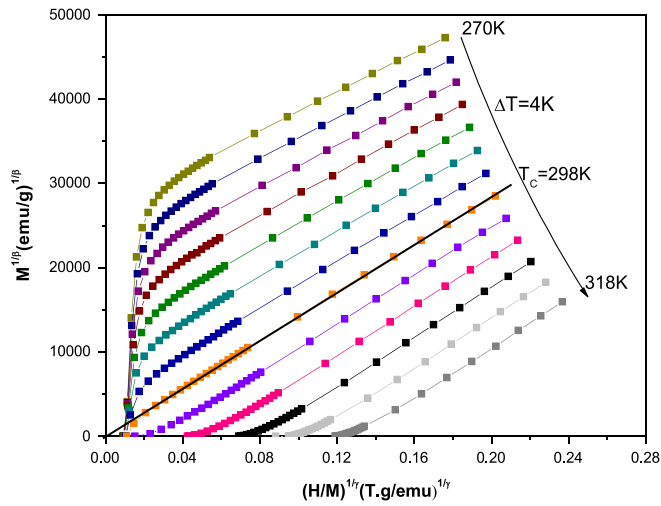


Fig. 4. Modified Arrott plots ($M^{1/\beta}$ vs. $(H/M)^{1/\gamma}$) using 3D-Heisenberg model exponents.

At T_C , the exponent δ relates magnetization M and applied magnetic field H by

$$M = D(H)^{1/\delta}, \quad t = 0 \quad (3)$$

here $M_s(T)$, is the spontaneous magnetization, $\chi_0^{-1}(T)$ is the inverse of magnetic susceptibility, t is reduced temperature $t = T - T_C / T_C$; and M_0 , h_0 and D are the critical amplitudes. In order to determine the type of magnetic phase transition of $\text{AMn}_{0.9}\text{V}_{0.1}\text{O}_3$ sample, Arrott plots (M^2 vs. H/M) are constructed. An inspection of the sign of the slope of the isotherms of H/M vs. M^2 will give the nature of the phase transition: positive for second order and negative for first order. For the present sample, a second order phase transition has been confirmed with the positive slope of H/M vs. M^2 curve. According to the mean-field theory near T_C , H/M vs. M^2 at various temperatures should show a series of parallel lines. The line at $T = T_C$ should pass through the origin. The curves

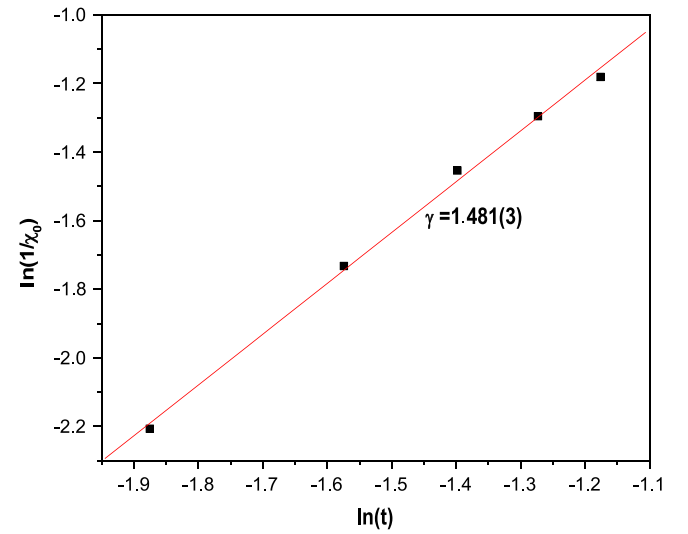
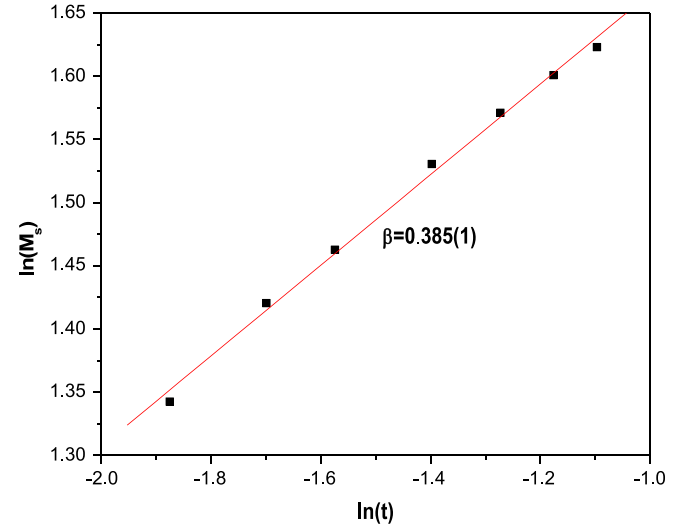


Fig. 5. \ln – \ln plot used to obtain the final values of β and γ .

in the Arrott plots are not linear suggests the non validity of mean-field theory. Therefore the data was analyzed using modified Arrott plot ($(H/M)^{1/\gamma}$ vs. $M^{1/\beta}$). This is given by the following equation of state [17]:

$$(H/M)^{1/\gamma} = a(T - T_C)/T + bM^{1/\beta} \quad (4)$$

where a and b are considered to be constants.

Different values of β and γ were taken as trial exponents (from 3D Heisenberg model, 3D Ising model and mean field model) for the construction of the modified Arrott plot.

In Fig. 4, we presented the modified Arrott plots $M^{1/\beta}$ vs. $(H/M)^{1/\gamma}$ constructed from the M vs. H plots at different temperatures by using the critical exponents $\beta = 0.365$ and $\gamma = 1.336$ similar to those of three-dimensional (3D) Heisenberg magnets. This plot clearly shows that the isotherms are a set of parallel straight in high magnetic fields. The intercepts of the isotherms on the x and y axes are $(1/\chi)^{1/\gamma}$ for $t \geq 0$ and $M_s^{1/\beta}$ for $t \leq 0$. From these initial values, linear fits to the isotherms are made to get the intercepts giving $M_s(T)$ and $\chi_0(T)$ and an initial value of T_C was determined from the isotherm that pass through

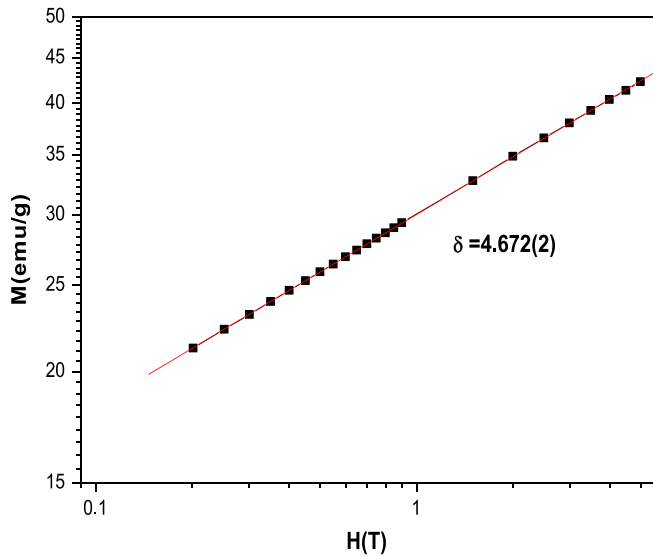


Fig. 6. $\ln(M)$ vs. $\ln(H)$ plot for $\text{La}_{0.6}\text{Nd}_{0.1}(\text{CaSr})_{0.3}\text{Mn}_{0.9}\text{V}_{0.1}\text{O}_3$ at $T = T_C$.

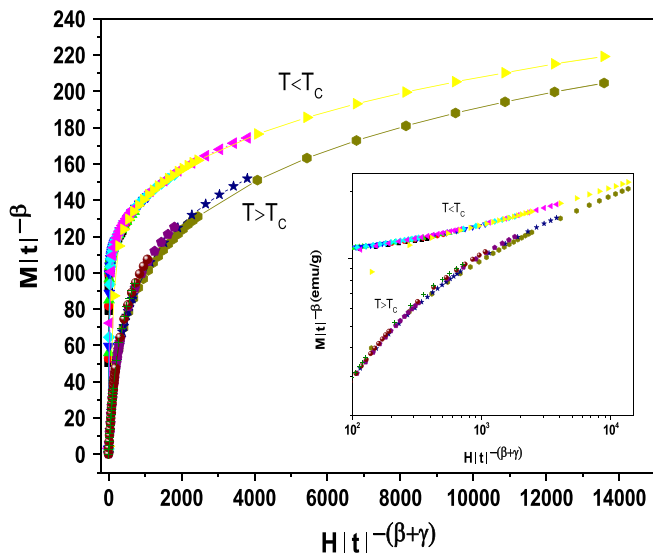


Fig. 7. Scaling plots below and above T_C using β and γ exponents determined from the modified Arrott method (only some typical curves are shown). The inset shows the same plots on a log–log scale.

the origin. A new value of β was obtained from $\ln(M_s)$ vs. $\ln(t)$ plot by fitting the data to a straight line, the slope of which gives. Similarly a new value of γ was obtained from the slope of $\ln(1/\chi)$ vs. $\ln(t)$ plot. The plots of $\ln(M_s)$ vs. $\ln(t)$ and $\ln(1/\chi_0)$ vs. $\ln(t)$ of our sample are shown in Fig. 5, where the obtained values of β and γ are also shown respectively. The final obtained values are $T_C = 298$ K, $\beta = 0.385(1)$ and $\gamma = 1.481(3)$. Concerning the value of δ , it can be determined directly from the slope of $\ln(M)$ vs. $\ln(H)$ plot at T_C which is shown in Fig. 6, i.e. $\delta = 4.672(2)$. Three exponents β , γ and δ derived from our statics scaling analysis are related by the Widom scaling relation [18]

$$\delta = 1 + (\gamma/\beta) \quad (5)$$

Using the values of β and γ , which were estimated from Fig. 6, in the above relation, we obtain $\delta = 4.846$. This value is close to that obtained from the critical isotherms at T_C , for our composition studied. Thus, the estimates of the critical exponents are consistent. In the critical region, the magnetization and applied magnetic field should obey the universal scaling behavior.

In Fig. 7, we show the plots of $M|t|^{-\beta}$ vs. $H|t|^{-(\beta+\gamma)}$ for $\text{AMn}_{0.9}\text{V}_{0.1}\text{O}_3$. The two curves represent temperatures below and above T_C . The inset shows the same data on a log–log plot. It can be clearly seen that all the points fall on two curves, one for $T < T_C$ and another one for $T > T_C$. This corroborates that the obtained values of the critical exponents and T_C are reliable and in agreement with the scaling hypothesis.

3.4. Magnetocaloric effect

This part deals with the magnetocaloric effect and the influence of critical exponents on the field dependence of entropy change of polycrystalline $\text{AMn}_{0.9}\text{V}_{0.1}\text{O}_3$ sample.

The magnetocaloric effect can be characterized by the magnetic entropy change due to the application of a magnetic field H . This entropy change can be evaluated by processing the temperature and field dependent magnetization curves

$$\Delta S_M(T, H) = S_M(T, H) - S_M(T, 0) = \int_0^H \left(\frac{\partial M}{\partial T} \right)_H dH \quad (6)$$

In the case of magnetization measurements at small discrete field and temperature intervals, ΔS_M can be approximated from Eq. (6) by

$$\Delta S_M \left(\frac{T_1 + T_2}{2} \right) = \left(\frac{1}{T_2 - T_1} \right) \left[\int_0^{H_{\max}} M(T_2, H) dH - \int_0^{H_{\max}} M(T_1, H) dH \right] \quad (7)$$

Fig. 8 shows the temperature dependence of the magnetic entropy change for $\text{AMn}_{0.9}\text{V}_{0.1}\text{O}_3$ up to 5 T computed from Eq. (7) using the measured magnetization data. The obtained curves are similar to those of other perovskite manganites [19–21]. ΔS_M reaches a maximum value in the vicinity of T_C . The value of ΔS_M peak increases with the field and the peak position remain nearly unaffected. At a magnetic field of 5 T, the maximum value of entropy change (ΔS_M) is found to be about 4.23 J/kg K at 300 K. The temperature at which maximum entropy change observed are in good agreement with T_C obtained from the M vs. T curves.

The magnetocaloric effect in manganites always focus on a temperature window centered about the Curie temperature, the critical exponents influences the nature of magnetic caloric response [22]. In order to demonstrate this coupling, the field dependence of entropy change is analyzed. According to Oesterreicher et al., the field dependence of the magnetic entropy change (ΔS_M) of materials with a second order phase transition can be expressed as

$$\Delta S_M \propto H^n \quad (8)$$

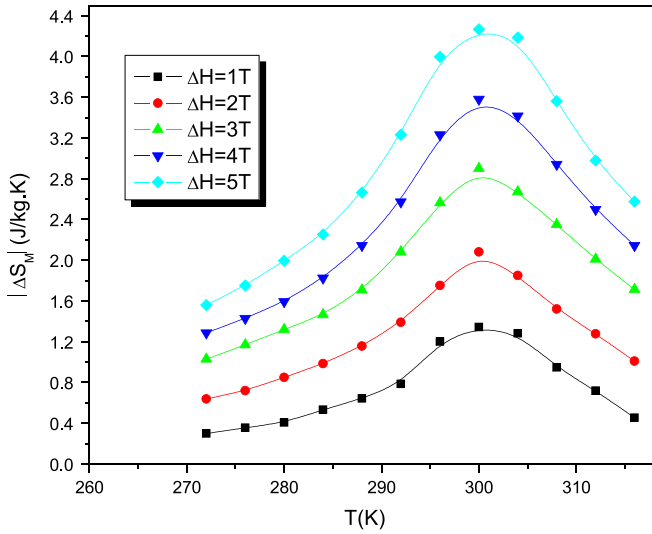


Fig. 8. Temperature dependence of the magnetic entropy change (ΔS_M) at different applied magnetic field change interval for $\text{La}_{0.6}\text{Nd}_{0.1}(\text{CaSr})_{0.3}\text{Mn}_{0.9}\text{V}_{0.1}\text{O}_3$.

where the exponent n depends on the magnetic state of the compound. It can be locally calculated as follows:

$$n = \frac{d \ln \Delta S_M}{d \ln H} \quad (9)$$

In the particular case of $T = T_C$ or at the temperature of the peak entropy change, the exponent n becomes field independent [23]. In this case

$$n(T_C) = 1 + \frac{\beta - 1}{\beta + \gamma} \quad (10)$$

where β and γ are the critical exponents.

With, $\beta\delta = (\beta + \gamma)$ the relation (10) can be written as

$$n(T_C) = 1 + \frac{1}{\delta} \left(1 - \frac{1}{\beta} \right) \quad (11)$$

Using the order parameters ($\beta = 0.385(1)$, $\gamma = 1.481(3)$ and $\delta = 4.672(2)$ at $T_C = 298$ K), obtained from the modified Arrott plot method, the values of n calculated from the above relations are found to be 0.687 (from Eq. (10)) and 0.658 (from Eq. (11)) for our sample. These values are lower than the mean field predictions $n = 2/3$ [24]. The deviation from the mean field behavior is due to the presence of local inhomogeneities in the vicinity of transition temperature [25]. Otherwise, the exponent n can be also calculated directly from the fitting of the linear plot of ΔS_M vs. H constructed at the transition temperature of the peak of the magnetic entropy change i.e., at 300 K which is shown in Fig. 9. The value of n obtained from the slope is 0.728(3), which are in good agreement with that obtained from the critical exponents using the modified Arrott plot method (from Eqs. (10) and (11)).

3.5. Relative cooling power

Another useful parameter which decides the efficiency of a magnetocaloric material is the RCP or the refrigerant capacity. It is the heat transfer between the hot and the cold reservoirs

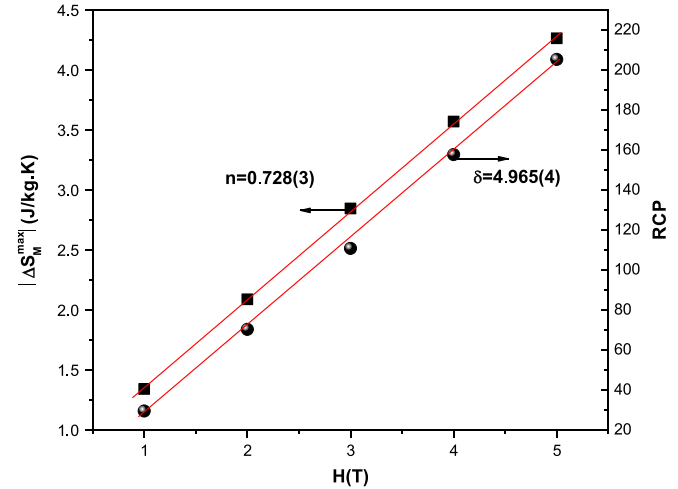


Fig. 9. Field dependence of entropy change and RCP for $\text{La}_{0.6}\text{Nd}_{0.1}(\text{CaSr})_{0.3}\text{Mn}_{0.9}\text{V}_{0.1}\text{O}_3$ at 300 K. The lines indicate non-linear curve fitting of the data.

during an ideal refrigeration cycle. This represent numerically the area under $-\Delta S_M$ vs. T curve

$$\text{RCP} = -\Delta S_M^{\text{max}} \times \partial T_{\text{FWHM}} \quad (12)$$

where ∂T_{FWHM} is the full width at half maximum of the magnetic entropy change curve.

The estimated value of RCP is found to be 205.35 J kg^{-1} . This value is about 49.72% of that of the Gadolinium Gd at 294 K for $\Delta H = 5 \text{ T}$ [26]. Therefore, these materials can be considered as potential candidate for magnetic cooling applications.

The field dependence of RCP, for our sample is analyzed. It can be expressed as a power law by taking account of the field dependence of entropy change ΔS_M and reference temperature into consideration [12] i.e.

$$\text{RCP} \propto H^{1+1/\delta} \quad (13)$$

where δ being the critical exponent of the magnetic transition.

Field dependence of RCP is depicted in Fig. 9. The value δ calculated from the exponent is 4.965(4) for the sample. This is in agreement with that obtained using modified Arrott plot and Widom scaling relation.

4. Conclusion

We prepared a perovskite manganite sample $\text{AMn}_{0.9}\text{V}_{0.1}\text{O}_3$ and then studied the critical behavior and magnetic entropy change around T_C . Arrott plots reveal second order nature of magnetic transition in the compound. The critical exponents analysis using the modified Arrott method yields $\beta = 0.358(1)$; $\gamma = 1.481(3)$; $\delta = 4.672(2)$ and $T_C = 298$ K for our compound. The value of the critical exponents are quite close to values expected for the universality class of 3D Heisenberg ferromagnets with short-range interaction. The field dependence of the magnetic entropy change is also analyzed, showing the power law dependence $\Delta S_M \propto H^n$ where $n = 0.728(3)$ at 300 K for the compound at their respective transition temperature. Broad operating temperature range along with moderate values

of ΔS_M and RCP make of $\text{AMn}_{0.9}\text{V}_{0.1}\text{O}_3$ a potential candidate for room temperature magnetic refrigeration.

References

- [1] X. Zhang, B. Zhang, S. Yu, Z. Liu, W. Xu, G. Liu, *Physical Review B* 76 (2007) 132403.
- [2] J. Du, Q. Zeng, Y.B. Li, Q. Zhang, D. Li, Z.D. Zhang, *Journal of Applied Physics* 103 (2008) 023948.
- [3] M.H. Phan, M.B. Mrales, N.S. Bingham, H. Srikanth, *Physical Review B* 81 (2010) 094413.
- [4] J.L. Alonso, L.A. Fernández, F. Guinea, V. Laliena, V. Martín-Mayor, *Nuclear Physics B* 596 (2001) 587.
- [5] A.K. Pramanik, A. Banerjee, *Physical Review B* 79 (2009) 214426.
- [6] J.L. Dormann, D. Fiorani, E. Tronc, *Advances in Chemical Physics* 98 (1997) 283.
- [7] X. Batlle, A. Labarta, *Journal of Applied Physics* 35 (2002) R15.
- [8] J. Fan, L. Ling, B. Hong, L. Zhang, L. Pi, Y. Zhang, *Physical Review B* 81 (2010) 144426.
- [9] K. Ghosh, C.J. Lobb, R.L. Greene, S.G. Karabashev, D.A. Shulyatev, A.A. Arsenov, Y. Mukovskii, *Physical Review Letters* 81 (1998) 4740.
- [10] J. Yang, Y.P. Lee, Y. Li, *Physical Review B* 76 (2007) 054442.
- [11] R. caballero-Flores, V. Franco, A. Conde, L.F. Kiss, *Journal of Applied Physics* 108 (2010) 073921.
- [12] V. Franco, A. Conde, *International Journal of Refrigeration* 33 (2010) 465.
- [13] Zhiming Wang, Qingyu Xu, Kaixin Chen, *Current Applied Physics* 12 (2012) 1153.
- [14] A. Dhahri, F.I.H. Rhouma, J. Dhahri, E. Dhahri, M.A. Valente, *Solid State Communications* 151 (2011) 738.
- [15] H.M. Rietveld, *Journal of Applied Crystallography* 2 (1969) 65.
- [16] H.E. Stanley, *Introduction to Phase Transitions and Critical Phenomena*, Oxford University Press, London, 1971.
- [17] A. Arrott, J.E. Noakes, *Physical Review Letters* 19 (1967) 786.
- [18] B. Widom, *Journal of Chemical Physics* 41 (1964) 163.
- [19] A. Dhahri, J. Dhahri, E.K. Hlil, E. Dhahri, *Journal of Alloys and Compounds* 530 (2012) 1.
- [20] M. Khelifi, M. Bejar, O.E.L. Sadek, E. Dhahri, M.A. Ahmed, E.K. Hlil, *Journal of Alloys and Compounds* 509 (2011) 7410.
- [21] A. Omri, M. Bejar, M. Sajieddine, E. Dhahri, E.K. Hlil, M. Es-Souni, *Physica B* 407 (2012) 2566.
- [22] H.S. Shin, J.E. Lee, Y.S. Nam, H.L. Ju, C.W. Park, *Solid State Communications* 118 (2001) 377.
- [23] V. Franco, A. Conde, M.D. Kuz'min, J.M. Romero-Enrique, *Journal of Applied Physics* 105 (2009) 07A917.
- [24] M. Pekaa, *Journal of Applied Physics* 108 (2010) 113913.
- [25] Q.Y. Dong, H.W. Zhang, J.R. Sun, B.G. Shen, V. Franco, *Journal of Applied Physics* 103 (2008) 1161.
- [26] M.H. Phan, S.C. Yu, *Journal of Magnetism and Magnetic Materials* 308 (2007) 325.